RIS-Aided Polarization Aware Optimal WPT

Srishti Sharma and Swades De

Department of Electrical Engineering and Bharti School of Telecommunication

Indian Institute of Technology Delhi, New Delhi 110016, India

Abstract—This paper characterizes the impact of polarization on sustainable wireless power transfer (WPT) to the mobile Internet-of-Thing (IoT) devices, focusing on various transmitter and receiver antenna polarization states. It investigates both line-of-sight (LOS) and controlled non-LOS (NLOS) reflections via reconfigurable intelligent surface (RIS), deriving closed-form expressions for received power to identify optimal antenna polarization. Theoretical findings are experimentally validated in an anechoic chamber, showing strong agreement with a normalized root mean square error ≤ 0.08. The research also assesses the necessity of RIS's polarization handling, concluding its non-essentiality in single source-receiver setups. Simulations reveal that horizontal polarization boosts received power by $\geq 28\%$ compared to other polarizations. Furthermore, incorporating RIS in green communication significantly enhances received power.

Index Terms—Polarization beamforming, reconfigurable intelligent surface (RIS), wireless power transfer (WPT)

I. INTRODUCTION

WPT aligns with green communication by minimizing battery replacements through controlled, on-demand power delivery to devices. However, signal propagation is often hindered by obstacles creating multiple paths with varying amplitude, phase, and polarization, leading to significant weakening of received signal due to destructive interference between LOS and NLOS components. Mitigating this necessitates maximized constructive interference at the receiver via phase [1] and polarization [2] beamforming. However, signal depolarization deteriorates the system performance in weak LOS environment [3] or where a considerable transfer occurs through the NLOS channel [4]. Therefore, countering depolarization is crucial for enhancing WPT efficiency.

The concept of green communication-infused WPT finds use in charging or data transfer application to the obscurely deployed Internet-of-Thing (IoT) nodes. The key benefit results from the reduction of payload at the charger node by the virtue of reduction in transmit power. A fundamental research methodology involved phased array transmitter antenna design to generate a high-powered beam in the desired direction [5]. However, radiation of high-powered beams is constrained by Federal Communications Commission safety standards [6], resulting in insufficient performance of systems requiring high received power. To mitigate the propagation-based losses, strategies such as, beamforming [7], waveform design [1], and transmit diversity [8] were suggested.

Another major direction of research in green communication has been revolving around the use of RIS technology for compensating the propagation losses. A self-sustainable RIS-aided WPT scheme to improve the power transfer efficiency

and energy utility was suggested in [9]. To further enhance the received power, the study in [10] substituted the ground surface with RIS, thereby achieving a more focused beam. Though the channel-induced impairments in the phase of the transmit signal has been addressed by the methods proposed in the aforecited literature, the key aspect of polarization mismatch has remained uninvestigated.

Experimental demonstrations suggest the possibility of 10-20 dB SNR enhancement through polarization synchronization [11]. This has led to a greater focus on polarization-based power enhancements in the paradigm of sustainable communication, which could prove especially helpful in mobile networks. The conventional two-ray propagation model does not take polarization into account. To address the lacuna of impact of polarization and possible misalignment mitigation strategies, the preliminary work in [12] demonstrated the effect of polarization on the received signal power. However, the analysis was restricted to linear polarization (LP) and did not provide any means to maximize the received power. As an advance, this paper incorporates RIS to enhance the received power in a mobile networks and investigates optimum state of polarization (SOP) for WPT purposes over short distances.

At radio frequencies (RF), LOS signal is always accompanied by multipath components. Polarization change is maximum owing to reflection. Furthermore, the first-order reflection components may stay strongly polarized and have enough power to have a considerable impact on the received power. In light of this, the key contributions of this work are as follows:

1) A generalized mathematical characterization of received power for LOS, specular and controlled reflection is done, allowing easy adaptability of expressions over all SOP.
2) A geometrical investigation of effect of reflection on received power is used to determine the optimum SOP. Further, ability of optimum polarization state in enhancing WPT efficiency is experimentally verified.
3) Enhancement of received signal power is demonstrated via use of RIS-substituted ground plane.
4) It is proved that polarization handling capability is not required at the RIS in single transmitter-receiver scenario.

This work can be used in IoT device charging in obscure geometrical scenarios, drone-based information and power transfer, etc. Incorporation of polarization aspect further enhances the received gains. *We consider that the phases of received signals are aligned via RIS using technique in [13].*

Notations: Anti-clockwise rotation by angle γ about x, y, and z axes are denoted by $\mathbf{R}_x(\gamma)$, $\mathbf{R}_y(\gamma)$, and $\mathbf{R}_z(\gamma) \in \mathbb{R}^{3\times3}$ [14]. $|\cdot|$ is modulus operator and $(\cdot)$ is dot operator.
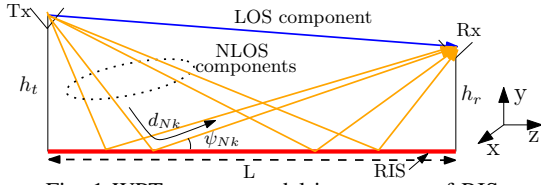
Fig. 1 WPT system model in presence of RIS.

II. Various WPT Scenarios

Fig. 1 depicts a snapshot (time $t = t_0$) of the system model for WPT involving single transmitter and a mobile receiver. The transmitter of height h_t is placed at a distance L from the receiver of height h_r. Receiver mobility is considered along z. The RIS is capable of controlling phase, thereby directing multipath components to the mobile receiver. Scenarios with no NLOS, specular NLOS, and significant NLOS components are evaluated considering without as well as with RIS.

A. WPT with only LOS component

As RF wireless communication and energy transfer applications are generally in far-field, the electric field is considered to be a plane wave [15]. The expression of electric field using an unmodulated carrier signal is given as

$$\mathbf{E}_L(d_L, t) = \frac{h_L}{d_L} \exp[j(\omega t - 2\pi d_L/\lambda)]\hat{\mathbf{a}}_L. \tag{1}$$

$h_L = \sqrt{\frac{P_t}{4\pi} G_{tL}(1 - \Gamma_t^2)\eta}$, $d_L = L^2 + (h_t - h_r)^2$ is path length of LOS link, $L = L_0 + vt_0$, where L_0 is its starting location, v is velocity, and t_0 is the time of observation, P_t is transmit power, G_{tL} is transmitter antenna gain in LOS direction, Γ_t is transmit antenna reflection coefficient, ω is angular frequency, λ is wavelength and $\hat{\mathbf{a}}_L$ is polarization of transmitted LOS field. The power at the receiver antenna is given as $P_r = |\mathbf{E} \cdot \mathbf{H}^*|^2/\eta$, where η is intrinsic impedance of free space. The effective vector height $\mathbf{H}$ of receiver antenna is given in [12] with polarization vector $\hat{\mathbf{a}}_r = q_x\hat{a}_x + q_y\hat{a}_y$, q_x and q_y may be complex depending on the receiver polarization. From Friis equation, power at far field distance d is [12]

$$P_r = P_t G_{tL} G_r (1 - |\Gamma_t|^2)(1 - |\Gamma_r|^2)(\lambda/4\pi d_L)^2 |\hat{\mathbf{a}}_L \cdot \hat{\mathbf{a}}_r|^2 \tag{2}$$

where G_r is the receive antenna gain and Γ_r is the reflection coefficient owing to load mismatch. From (2), for maximizing P_r, $|\hat{\mathbf{a}}_e \cdot \hat{\mathbf{a}}_r|^2 \to 1$, i.e., identical polarization of transmitter and receiver antennas, as considered in the subsequent analysis.

For small d, power in NLOS components may be comparable to LOS component. Therefore, polarization misalignment may impact significantly, which is not accounted in (2). Next, we consider the effect of ground-reflected NLOS component.

Note. *All the derivations here onwards involve the receiver mobility through the velocity term incorporated in L.*

B. WPT with LOS and only specular NLOS component

In presence of LOS and NLOS components, surface irregularities present in the environment are negligible in comparision to the wavelength of radiating beam. Thus, only specular

reflected NLOS components is considered, resulting in a two-ray model. The received LOS field is given in (1). Let source polarization vector be $[p_x, p_y]^T$, polarization of LOS link is

$$\hat{\mathbf{a}}_L = \mathbf{R}_x(-\theta_L)[p_x \ p_y \ 0]^T = p_x\hat{a}_x + \cos\theta_L p_y\hat{a}_y - \sin\theta_L p_y\hat{a}_z. \tag{3}$$

$\theta_L = \tan^{-1}\left(\frac{h_t - h_r}{L}\right)$ is angle of arrival (AoA) of LOS signal. Impact of NLOS component depends on the gain in corresponding elevation and azimuth direction. The polarization vector of NLOS field is $\hat{\tilde{\mathbf{a}}}_N = p_x\hat{a}_x + \cos\theta_N p_y\hat{a}_y - \sin\theta_N p_y\hat{a}_z$ (obtained similarly as $\hat{\mathbf{a}}_L$), where $\theta_N = \tan^{-1}\left[\frac{h_t + h_r}{L}\right]$ is the angle of NLOS ray with z-axis. On interaction with the ground, reflected field polarization is impacted by its parallel ($\Gamma_\parallel$) and perpendicular ($\Gamma_\perp$) reflection coefficients [15] as

$$\hat{\mathbf{a}}'_N = \Gamma_\perp p_x\hat{a}_x + \Gamma_\parallel \cos\theta_N p_y\hat{a}_y - \Gamma_\parallel \sin\theta_N p_y\hat{a}_z. \tag{4}$$

Specular reflected component follows Snell's law of reflection, i.e., $\psi_N = \theta_N$. The NLOS field after ground reflection is

$$\mathbf{E}_N(d_N, t) = \frac{h_N}{d_N} \exp[j(\omega t - 2\pi d_N/\lambda)]\hat{\mathbf{a}}_N. \tag{5}$$

$h_N = \sqrt{\frac{P_t}{4\pi} G_{tN}(1 - \Gamma_t^2)\eta}$, G_{tN} is transmitter gain in NLOS component direction. Path length d_N of the NLOS link is given in [12]. From (4), the corresponding polarization vector is

$$\hat{\mathbf{a}}_N = \mathbf{R}_x(2\theta_N)\begin{bmatrix} \Gamma_\perp p_x & \Gamma_\parallel \cos\theta_N p_y & -\Gamma_\parallel \sin\theta_N \end{bmatrix}^T$$
$$= \Gamma_\perp p_x\hat{a}_x + \Gamma_\parallel \cos\theta_N p_y\hat{a}_y + \Gamma_\parallel \sin\theta_N p_y\hat{a}_z. \tag{6}$$

The total field at the receiver is $\mathbf{E}_T = \mathbf{E}_L + \mathbf{E}_N$. Using (1) and (5), total power at the receiver is

$$P_r = \left| \left(\frac{h_L g_L}{d_L\sqrt{\eta}} e^{j\left(\omega t - \frac{2\pi d_L}{\lambda}\right)}\hat{\mathbf{a}}_L + \frac{h_N g_N}{d_N\sqrt{\eta}} e^{j\left(\omega t - \frac{2\pi d_N}{\lambda}\right)}\hat{\mathbf{a}}_N \right) \cdot \hat{\mathbf{a}}_r^* \right|^2 \tag{7}$$

where $g_L = \sqrt{(1 - \Gamma_r^2)G_{rL}\frac{\lambda^2}{4\pi}}$ and $g_N = \sqrt{(1 - \Gamma_r^2)G_{rN}\frac{\lambda^2}{4\pi}}$; G_{rL} and G_{rN} are the receiver antenna gains in LOS and NLOS directions, respectively. (7) provides a generic form of the two-ray model while accounting for arbitrary SOP.

Note that, without RIS, only specular reflection reaches the receiver. However, the NLOS components resulting from irregularities in the ground surface could majorly impact the WPT gain. Therefore, focus is to capture all the components at the receiver within at most one reflection. To achieve this, we consider RIS-substituted ground surface, as presented next.

C. RIS-aided WPT in presence of LOS and NLOS components

An RIS-substituted ground surface permits anomalous reflections which enable non-specular components to reach the receiver without significant attenuation. The received LOS field is still characterized by (1). A total of K NLOS components reach the receiver after being steered through the RIS. The E-field for the k-th NLOS component before reflection is

$$\tilde{\mathbf{E}}_{Nk}(\tilde{d}_{Nk}, t) = \frac{h_{Nk}}{\tilde{d}_{Nk}} \exp[j(\omega t - 2\pi \tilde{d}_{Nk}/\lambda)]\hat{\tilde{\mathbf{a}}}_{Nk} \tag{8}$$

where $\tilde{d}_{Nk}$ is the distance from transmitter to the k-th RIS element and the corresponding polarization vector is $\hat{\tilde{\mathbf{a}}}_{Nk} =$

$p_x \hat{a}_x + \cos\theta_{Nk} p_y \hat{a}_y - \sin\theta_{Nk} p_y \hat{a}_z$, where θ_{Nk} is the angle of k-th NLOS ray with z-axis. $h_{Nk} = \sqrt{\frac{P_t}{4\pi} G_{tNk}(1-\Gamma_t^2)\eta}$ in which G_{tNk} is gain in direction of k-th NLOS link. *In this work, we consider negligible contribution due to the out-of-plane reflections, which can be attributed to high distance-dependent losses due to extra path traversal and the additional AoA losses.* The k-th RIS element reflects the k-th NLOS component towards the receiver by imparting weight w_k to it. d_{Nk} is total path length of k-th NLOS link and is given as

$$d_{Nk} = \sqrt{h_t^2 + h_t^2/\tan^2\theta_{Nk}} + \sqrt{h_r^2 + (L - h_t/\tan\theta_{Nk})^2}. \quad (9)$$

To compute w_k we formulate the optimization problem as

$$(\mathbf{P}1): \quad \min_{w_k}(w_k\tilde{\mathbf{E}}_{Nk})^H\mathbf{H} \quad (10)$$
$$\mathbf{C}11: \quad \|w_k\|_F = \mathbf{1}.$$

Constraint $\mathbf{C}11$ ensures that the RIS imparts no additional gain to the reflected ray. The objective problem ($\mathbf{P}1$) aims to reduce the losses due to the misalignment between the receiver and the received polarization of the reflected or direct component(s).

Lemma 1. *The optimal weight imparted by the RIS is*

$$w_k^* = e^{j\kappa_{Nk}^*}\boldsymbol{R}_x\left((\tan^{-1}(h_t/x_{Nk}) + \tan^{-1}(h_r/(L - x_{Nk})))\right)$$

Proof. The weight assumes the form $w_k = e^{j\kappa_{Nk}}\mathbf{R}_x(\theta_{Nk} + \psi_{Nk})$, where κ_{Nk} is the additional phase offset imparted by the RIS element to compensate the phase difference between the LOS and the NLOS component(s). ψ_{Nk} denotes the angle which the k-th reflected ray makes with RIS element in order to reach receiver as shown in Fig. 1. This phase offset κ_{Nk}^* can be computed using the studies in [10], [13]. Adopting a geometrical optimization approach to determine the optimal values of ψ_{Nk} and θ_{Nk} we get, $\psi_{Nk} = \tan^{-1}\frac{h_r}{L - x_{Nk}}$, and $\theta_{Nk} = \tan^{-1}\frac{h_t}{x_{Nk}}$, where x_{Nk} is the distance of k-th RIS element from the base of the transmitter. Therefore, the optimal weight imparted by the k-th RIS element is w_k^*. $\quad\square$

As consideration of losses in the reflective element of RIS is beyond the scope of this article, the RIS is considered to perfectly reflect both parallel and perpendicular polarized signals. Hence, using Lemma 1, received k-th NLOS field is

$$\mathbf{E}_{Nk}(d_{Nk}, t) = \frac{h_{Nk}}{d_{Nk}}\exp[j(\omega t - 2\pi d_{Nk}/\lambda + \kappa_{Nk}^*)]\hat{\mathbf{a}}_{Nk}, \quad (11)$$

where $\hat{\mathbf{a}}_{Nk} = p_x\hat{a}_x + \cos\psi_{Nk} p_y\hat{a}_y + \sin\psi_{Nk} p_y\hat{a}_z$. Therefore, total electric field at receiver is $\mathbf{E}_T = \mathbf{E}_L + \sum_{k=1}^K \mathbf{E}_{Nk}$. Thus, the total received power after phase correction at the RIS is

$$P_r = \left|\left(\frac{h_L g_L}{d_L\sqrt{\eta}}\hat{\mathbf{a}}_L + \sum_{k=1}^K \frac{h_{Nk} g_{Nk}}{d_{Nk}\sqrt{\eta}}\hat{\mathbf{a}}_{Nk}\right)\cdot\hat{\mathbf{a}}_r^* e^{j\left(\omega t - \frac{2\pi d_L}{\lambda}\right)}\right|^2 \quad (12)$$

where $g_{Nk} = \sqrt{(1 - \Gamma_r^2)G_{rNk}\frac{\lambda^2}{4\pi}}$, G_{rNk} is the receiver antenna gain of k-th NLOS component. (12) indicate that after phase matching the received power solely depends on the polarization of the received fields and receiver antenna.

Remark 1. *The optimization in* (10), *with the objective to minimize the misalignment based losses, is not limited to the*

system described in Fig. 1. It is evident that the optimization objective, if applied to any source-receiver arrangement (in any number or geometry), would enhance the received power.

III. IMPACT OF TRANSMITTER AND RECEIVER SOP

In practical settings, communication antennas are generally LP or circularly polarized (CP) [3]. This research focuses on short-range WPT performance with typical antenna pairings such as vertical, horizontal, circular, and dual-LP. Vertical antennas are utilized in AM radio and vehicle antennas, horizontal in TV broadcasting, circular in satellite communications, and dual-LP in scenarios with varying receiver polarizations like cellular and Wi-Fi networks.

The research, detailed in Table I, assesses the polarization vectors for LOS and NLOS fields and receiver antennas, alongside total received power in each case. It finds that vertical polarization is prone to setup-related losses, while horizontal polarization effectively retains both LOS and NLOS components without loss. CP, despite its losses, is advantageous over vertical due to its orthogonal transmission. RIS plays a critical role in enhancing efficiency by counteracting the π phase shift and averting changes in polarization from left-hand circularly polarized (LHCP) to right-hand circularly polarized (RHCP), improving system performance. The findings highlight that horizontal polarization provides the most significant gain, merging specular and controlled NLOS elements.

Claim 1. *No correction of polarization is required at the RIS in single source-receiver WPT scenario.*

Proof. Here, we use contradiction. Any polarization can be broken down into orthogonal components. Our study shows that horizontal polarization remains unaffected at the receiver, but vertical polarization (in vertical, circular, or dual-linear polarized antennas) incurs losses. We need to explore if a more effective vertical polarization orientation exists for RIS implementation. With vertically polarized transmitter and receiver, the polarization of the field at RIS is $[0, \cos\theta_{Nk}, -\sin\theta_{Nk}]^T$. Suppose RIS adds a rotation of γ to θ_{Nk} to optimize received power. Each RIS element adjusts the NLOS component's polarization using the rotation matrix in (13). The rotated NLOS field polarization vector is $[-\sin\gamma, \cos\psi_{Nk}\cos\gamma, \sin\psi_{Nk}\cos\gamma]^T$, and $\mathbf{a}_r = [0, 1, 0]^T$. For optimal polarization absorption, $\cos\psi_{Nk}\cos\gamma$ must be maximized, achievable only when $\gamma = 0$.

$$\begin{bmatrix} \cos\gamma & -\sin\gamma\cos\theta_{Nk} & \sin\gamma\sin\theta_{Nk} \\ \cos\theta_{Nk}\sin\gamma & \left\{\begin{array}{c}\cos^2\theta_{Nk}\cos\gamma \\ +\sin^2\theta_{Nk}\end{array}\right\} & \left\{\begin{array}{c}\sin\theta_{Nk}\cos\theta_{Nk} \\ \times(1-\cos\gamma)\end{array}\right\} \\ -\sin\gamma\sin\theta_{Nk} & \left\{\begin{array}{c}\sin\theta_{Nk}\cos\theta_{Nk} \\ \times(1-\cos\gamma)\end{array}\right\} & \left\{\begin{array}{c}\sin^2\theta_{Nk}\cos\gamma \\ +\cos^2\theta_{Nk}\end{array}\right\} \end{bmatrix} \quad (13)$$

$\square$

Remark 2. *In single source WPT, phase corrective RIS along with horizontal source and receiver polarization leads to maximum beamforming gain. Notably, the aim of the presented analysis is to benchmark the possible gain that can be attained by concentrating NLOS component towards the receiver.*

TABLE I Received power for different sets of polarization

Antenna combinations	Polarization	Received power
Both transmitter and receiver are vertically polarized	$\hat{\mathbf{a}}_L = \cos\theta_L \hat{a}_y,$ $\hat{\mathbf{a}}_{Nk} = \cos\psi_{Nk}\hat{a}_y,\ \hat{\mathbf{a}}_r = \hat{a}_y$	$P_r = \left(\dfrac{h_L g_L}{d_L\sqrt{\eta}}\cos\theta_L + \sum_{k=1}^{K}\dfrac{h_{Nk}g_{Nk}}{d_{Nk}\sqrt{\eta}}\cos\psi_{Nk}\right)^2$
Both transmitter and receiver are horizontally polarized	$\hat{\mathbf{a}}_L=\hat{\mathbf{a}}_{Nk}=\hat{a}_x,$ $\hat{\mathbf{a}}_r = \hat{a}_x$	$P_r = \left(\dfrac{h_L g_L}{d_L\sqrt{\eta}} + \sum_{k=1}^{K}\dfrac{h_{Nk}g_{Nk}}{d_{Nk}\sqrt{\eta}}\right)^2$
Both transmitter and receiver are circularly polarized	$\hat{\mathbf{a}}_L=1/\sqrt{2}e^{j\frac{\pi}{2}}\hat{a}_x+\cos\theta_L/\sqrt{2}\hat{a}_y,$ $\hat{\mathbf{a}}_{Nk}=1/\sqrt{2}e^{j\frac{\pi}{2}}\hat{a}_x+\cos\psi_{Nk}/\sqrt{2}\hat{a}_y,$ $\hat{\mathbf{a}}_r=1/\sqrt{2}e^{j\frac{\pi}{2}}\hat{a}_x+1/\sqrt{2}\hat{a}_y$	$P_r=\left(\dfrac{h_Lg_L(1+\cos\theta_L)}{2d_L\sqrt{\eta}}+\sum_{k=1}^{K}\dfrac{h_{Nk}g_{Nk}(1+\cos\psi_{Nk})}{2d_{Nk}\sqrt{\eta}}\right)^2$
Transmitter is dual linear-polarized and receiver is circularly polarized	$\hat{\mathbf{a}}_L=1/\sqrt{2}\hat{a}_x + 1/\sqrt{2}\cos\theta_L\hat{a}_y,$ $\hat{\mathbf{a}}_{Nk}=1/\sqrt{2}\hat{a}_x+\cos\psi_{Nk}/\sqrt{2}\hat{a}_y,$ $\hat{\mathbf{a}}_r=1/\sqrt{2}e^{j\frac{\pi}{2}}\hat{a}_x+1/\sqrt{2}\hat{a}_y$	$P_r = \left(\dfrac{h_Lg_L\cos\theta_L}{2d_L\sqrt{\eta}} + \sum_{k=1}^{K}\dfrac{h_{Nk}g_{Nk}\cos\psi_{Nk}}{2d_{Nk}\sqrt{\eta}}\right)^2$ $+ \left(\dfrac{h_Lg_L}{2d_L\sqrt{\eta}} + \sum_{k=1}^{K}\dfrac{h_{Nk}g_{Nk}}{2d_{Nk}\sqrt{\eta}}\right)^2$

TABLE II Parameters for experimental setup

Parameter	Value	Parameter	Value
P_t	20 dBm	$(\Gamma_\parallel)_{Al}$	1
h_t	1.05 m	$(\Gamma_\perp)_{Al}$	-1
h_r	0.76 m	λ	0.3276 m
L	1.54 m	G_{omni}	1 dBi
Cable loss	8.08 dBm	G_{dir}	6.1 dBi
$(\Gamma_t, \Gamma_r)_{omni}$	0.8462	$(\Gamma_t, \Gamma_r)_{dir}$	1

IV. RESULTS AND DISCUSSION

This section confirms the proposed optimum polarization through experimental and simulation outcomes. The experiment, conducted in an anechoic chamber, included components like the Hittite generator HMC-T2100 (RF source), Keysight N9010A EXA (spectrum analyzer), and aluminum foil as a reflector to mimic the ground plane ($\epsilon_r \to \infty$). Both omnidirectional and directional (Powercast 915 MHz) antennas were used, with gains detailed in [15]. MATLAB simulations were compared with Section II's numerical results and experimental data. Here, $0°$ and $90°$ denote horizontal and vertical polarization, respectively, measured from the x-axis. Experiments at 915 MHz validated numerical findings, chosen due to the limited experimental setup and component compatibility at this frequency. For practical RIS demonstrations in the GHz range [16], simulations at 5 GHz were aligned with numerical expressions within acceptable simulation error margins, thus validating our analytical models experimentally and via simulations. Note, the operation range is influenced by the transmitter and receiver's mounting height.

A. Experimental validation

Experiment (setup in Fig. 2, parameter values in Table II) was conducted in two settings: 1) without ground reflector (only LOS), and 2) with ground reflector (with NLOS components), using two type of antennas. Transmit and receive antenna polarization were kept identical for maximum power transfer. Experimental data was collected by rotating antennas from $0°$ to $90°$ with $15°$ step size. Without reflector, polarization angle showed little or no impact on received power. With reflector located along the path between transmitter and receiver, multiple NLOS components potentially contribute to the received power. The experimental results in Figs. 3(a) and (b) indicate that horizontal polarization outperforms vertical. This is consistent with the results in Section II.

Assuming the source and receiver polarization orientation angle α, and substituting $p_x=q_x=\cos\alpha$ and $p_y=q_y=\sin\alpha$
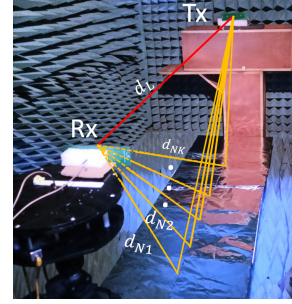
Fig. 2 Experimental setup having LOS and NLOS components.

TABLE III NRMSE between analytical and experimental values.

Setup	NRMSE	
	Fig. 3(a)	Fig. 3(b)
No reflector (Friss)	0.046	0.0545
Metal reflector	0.0726	0.0783

into (12), the normalized root mean square error (NRMSE) between numerical and experimental findings are shown in Table III (acceptable limit: NRMSE<0.08 [17]). This confirms the validity of (12). Experiments using omnidirectional and directional antennas, with 21 and 45 NLOS counts respectively, resulted in NRMSE ≤ 0.08. The gain ratio of LOS and NLOS, for directional antennas, is higher than for omnidirectional due to their emission patterns, allowing more significant NLOS components to affect received power. Phase synchronization of NLOS components with LOS link via RIS can further enhance the received signal. The analytical model remains same as Fig. 1, considering NLOS contributions only in the source-receiver plane. The small NRMSE values in Table III support our assumption of *negligible out-of-plane reflections*.

B. Simulation results

Parameters: $h_t=2$ m, $h_r=1.7$ m, $f=5$ GHz, $P_t=20$ dBm.
1) Specular NLOS component with ground reflection:
Initially, we explore the case without RIS, where only one specular component reaches the receiver. As detailed in Section II-B, this component depends on surface permittivity. Real permittivity values are used for practical RF comparisons due to negligible imaginary part at RF frequencies [18]. Examining the reflection coefficients' angle-dependence for ground plane [12], horizontal polarization is advantageous due to its higher reflection coefficient and AoA independence. Fig. 3(c) depicts received power variation with receiver mobility, captured through L, which impacts the phase mismatches
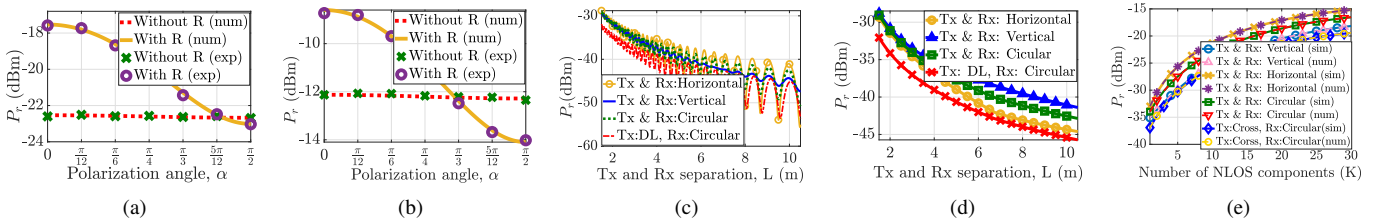
Fig. 3 Received power (*a*) with omnidirectional antenna, (*b*) with directional antenna, (*c*) without RIS, (*d*) with single RIS element, (*e*) with RIS-substituted ground; num: numerical, exp: experiment, R: reflector, DL: dual linear.

between LOS and NLOS components. Simulation results suggest that phase-matched horizontal polarization outperforms others, while vertical polarization shows least variation. This stability is due to small reflection coefficient and AoA, thus minimally affecting received power. CP and dual linear-CP display moderate performance. Fig. 3(*d*) presents the received power with phase-matched specular reflection, highlighting horizontal polarization's superiority under receiver mobility and the role of RIS in achieving the necessary phase matching.

2) Multiple NLOS components with RIS-substituted ground: Fig. 3(*e*) displays the received power for various source-receiver SOP at distance $L = 4$ m. Here, the NLOS and LOS components are phase-aligned by the RIS. Fig. 3(*e*) shows that horizontal polarization yields the highest power due to the absence of polarization loss. In contrast, combination of a dual LP transmitter and a CP receiver shows the least efficiency, as both LOS and k-th NLOS component diminish by $\cos \theta_L$ and $\cos \psi_{Nk}$ factor, respectively. This degradation varies based on the setup geometry. Notably, both CP and dual LP-CP configurations capture the orthogonal components, but the former outperforms due to identical SOP of source and receiver antennas. Circular, vertical, and dual LP-CP experience 29.548%, 53.958%, and 63.487% power reduction, respectively, compared to horizontal polarization. Moreover, Fig. 3(*e*) shows the advantages of using RIS: at $L = 4$ m, considering 10 and 30 NLOS components via RIS leads to received power gain of 95.99% and 99.02%, respectively, relative to a scenario with a single NLOS component.

Remark 3. *In single-source mobile WPT using ground reflection, horizontal polarization offers the best performance.*

V. Conclusion

This paper studied the power enhancement considering receiver mobility via polarization beamforming through RIS. It highlighted the impact of different SOP on WPT. Performance of the system is analyzed considering receiver mobility in various environmental settings, i.e., strong LOS, LOS with specular ground reflectivity, and the generic case of LOS with significant NLOS components. It is shown that horizontal polarization is optimum in the transmitter-RIS-receiver setting. We also verified the requirement of polarization handling capability in RIS by proposing polarization rotation matrix for the arbitrarily oriented antenna. We concluded that in single transmitter-receiver scenario, RIS is not required in polarization correction. Optimal source polarization is experimentally verified and the enhancement in received power with number

of RIS elements is verified by simulation. The findings related to the RIS-aided optimal polarization state are expected to play a useful role in efficient WPT in mobile IoT networks.

VI. Acknowledgement

References

[1] M. Vedady, *et al.*, "Waveform optimization for radio-frequency wireless power transfer : (invited paper)," in *Proc. 2017 IEEE 16th Int. Workshop Signal Process. Adv. Wireless Commun. (SPAWC)*, Dec. 2017, pp. 1–6.

[2] S. Sharma, *et al.*, "Impact of polarization on distributed optical beamforming," *IEEE Commun. Lett.*, vol. 27, no. 4, pp. 1180–1184, Feb 2023.

[3] C. Guo, *et al.*, "Advances on exploiting polarization in wireless communications: Channels, technologies, and applications," *IEEE Commun. Surv. Tutor.*, vol. 19, no. 1, pp. 125–166, Sept. 2017.

[4] I. Gaspard, "Polarization properties of the indoor radio channel," in *Proc. IEEE Int. Conf. Microw. Ant. Commun. Electron. Syst.*, 2015, pp. 1–5.

[5] X. Fan, *et al.*, "Energy-ball: Wireless power transfer for batteryless internet of things through distributed beamforming," *Proc. ACM Interact. Mob. Wearable Ubiquitous Technol.*, vol. 2, no. 2, p. 22, Jul. 2018.

[6] "FCC Rules and Regulations," ANSI Z136.1. [Online]. Available: https://www.air802.com/fcc-rules-and-regulations.html

[7] R. Mudumbai, G. Barriac, and U. Madhow, "On the feasibility of distributed beamforming in wireless networks," *IEEE Trans. Wirel. Commun.*, vol. 6, no. 5, pp. 1754–1763, May 2007.

[8] B. Clerckx and J. Kim, "On the beneficial roles of fading and transmit diversity in wireless power transfer with nonlinear energy harvesting," *IEEE Trans. Wirel. Commun.*, vol. 17, no. 11, pp. 7731–7743, 2018.

[9] Y. Cheng, *et al.*, "Self-sustainable RIS aided wireless power transfer scheme," *IEEE Trans. Veh. Technol.*, vol. 72, no. 1, pp. 881–892, 2023.

[10] E. Basar, *et al.*, "Wireless communications through reconfigurable intelligent surfaces," *IEEE Access*, vol. 7, pp. 116 753–116 773, 2019.

[11] A. Maltsev, *et al.*, "Impact of polarization characteristics on 60-GHz indoor radio communication systems," *IEEE Antennas Wirel. Propag. Lett.*, vol. 9, pp. 413–416, Apr. 2010.

[12] S. Sharma, *et al.*, "Effect of polarization on RF signal transmission over two-ray channel," in *Proc. Nat. Conf. Comm.*, Mar. 2023, pp. 1–6.

[13] A. Fascista, *et al.*, "RIS-aided joint localization and synchronization with a single-antenna receiver: Beamforming design and low-complexity estimation," *IEEE J. Sel. Top. Signal Process.*, vol. 16, no. 5, pp. 1141–1156, May 2022.

[14] E. Weisstein, "Rotation matrix," *https://mathworld. wolfram. com/*, 2003.

[15] S.Kumar, *et al.*, "RF energy transfer channel models for sustainable IoT," *IEEE IoT J.*, vol. 5, no. 4, pp. 2817–2828, Apr. 2018.

[16] Z. Zhang, *et al.*, "Active RIS vs. passive RIS: Which will prevail in 6G?" *IEEE Trans. Wirel. Commun.*, vol. 71, no. 3, pp. 1707–1725, 2023.

[17] D.Hooper, *et al.*, "Structural equation modeling: Guidelines for determining model fit," *The Elec. J. Bus. Res. Meth.*, vol. 6, 11 2007.

[18] I. Cuinas, *et al.*, "Depolarization due to scattering on walls in the 5 GHz band," *IEEE Trans. Antennas Propag.*, vol. 57, no. 6, pp. 1804–1812, 2009.